Carbon 102 (2016) 116–125

Contents lists available at ScienceDirect

Carbon

journal homepage: www.elsevier.com/locate/carbon

Knotted synthetic polymer or carbon nanotube microfibres with enhanced toughness, up to 1400 J/g

Federico Bosia [a], Emiliano Lepore [b], Noe T. Alvarez [c, d], Peter Miller [d], Vesselin Shanov [c, d], Nicola M. Pugno [b, e, f, *]

[a] Department of Physics and "Nanostructured Interfaces and Surfaces" Interdepartmental Centre, University of Torino, Via P. Giuria 1, 10125, Torino, Italy
[b] Laboratory of Bio-Inspired & Graphene Nanomechanics, Department of Civil, Environmental and Mechanical Engineering, University of Trento, Via Mesiano, 77, 38123 Trento, Italy
[c] Nanoworld Laboratories, Department of Biomedical, Chemical and Environmental Engineering, University of Cincinnati, Cincinnati, OH 45221, USA
[d] Department of Biomedical, Chemical and Environmental Engineering, University of Cincinnati, 2901 Woodside Drive, Cincinnati, OH 45221-0012, USA
[e] Center for Materials and Microsystems, Fondazione Bruno Kessler, Via Sommarive 18, 38123 Povo, Trento, Italy
[f] School of Engineering and Materials Science, Queen Mary University of London, Mile End Road, London E1 4NS, United Kingdom

ARTICLE INFO

Article history:
Received 18 November 2015
Received in revised form
6 February 2016
Accepted 8 February 2016
Available online 11 February 2016

ABSTRACT

In the past 50 years, a number of synthetic polymer microfibres, such as para-aramid or ultra-high-molecular-weight polyethylene, have been developed, exhibiting remarkable strength. However, their toughness is considerably smaller than that of some natural fibres such as spider silk, thus limiting their performance in applications ranging from surgical devices to vehicle parts. Here, we implement a recently proposed strategy, using micro-knots as frictional energy dissipators, to achieve record toughness values of up to 1400 J/g in synthetic microfibres, while maintaining their strength virtually unchanged. The same strategy is also applied to carbon nanotube microfibres, exploiting their superior ideal mechanical strength compared to any other existing fibre at the nanoscale, and toughness improvements of more than an order of magnitude are observed. We also show how knotted nanotube fibre configurations can be optimized for maximum toughness by modifying fibre diameter and twist angle, and how frictional and wear levels can be tuned by varying tightening and number of coils in the micro-knots. The results demonstrate the potential to design and produce fibres and textiles with unprecedented simultaneous strength and toughness for a variety of technological applications.

1. Introduction

It is known that many biological structural materials can effectively combine properties that are apparently mutually exclusive, or at least in strong competition, such as high stiffness and low density [1], or strength and toughness [2,3]. Teeth [4], mollusc shells [5] or crustaceans [6] display exceptional combinations of stiffness, strength, flaw tolerance and toughness, at present unrivalled by engineering materials. Spider or silkworm silk is another prime example of this, with a tensile strength comparable to that of high-grade alloy steels, and a toughness three times higher than even high energy-absorbing polymers such as Kevlar® [7,8]. This means that silk fibres are able to dissipate a huge (e.g. kinetic) energy before breaking. In Ref. [8], the toughest known biomaterial is discussed, namely the silk spun by a giant riverine orb spider, reaching energy-to-break values of 520 MJ/m^3, which is 10 times that of para-aramid synthetic fibres such as Kevlar®. In the case of artificial materials, Carbon NanoTubes (CNTs) provide excellent candidates to achieve superior mechanical properties [9,10], since their ideal mechanical strength is an order of magnitude greater than most commonly used industrial materials. The exceptional mechanical strength and low density of CNTs [11,12], similar to that of Graphene [13–15], evoke the possibility of futuristic projects such as the so-called "Space Elevator" [16,17]. However, the prospect of achieving these mechanical properties with the corresponding macroscopic fibres still presents a considerable challenge [18–20].

There is great interest in manufacturing fibre and film assemblies that attain on a macroscopic level the mechanical strength of individual CNTs. The ability to assemble CNTs into continuous fibres or threads (terms used indistinctly in CNT literature) has progressed considerably. Perhaps the most advanced methods to date

* Corresponding author. Laboratory of Bio-Inspired & Graphene Nanomechanics, Department of Civil, Environmental and Mechanical Engineering, University of Trento, Via Mesiano, 77, 38123 Trento, Italy.
E-mail address: nicola.pugno@unitn.it (N.M. Pugno).

http://dx.doi.org/10.1016/j.carbon.2016.02.025
0008-6223/

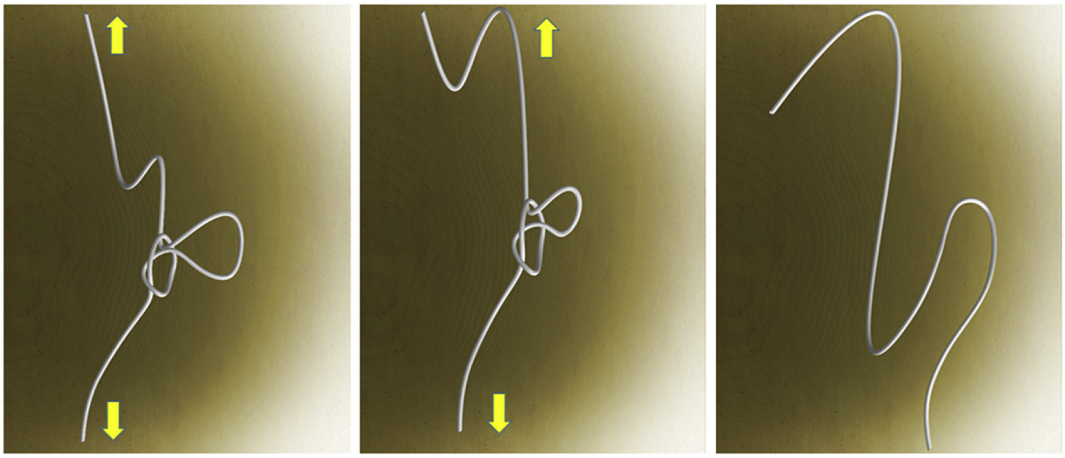

Fig. 1. Schematic of the overhand knot applied to the fibres and subsequent knot disentanglement after fibre pulling. Applied force is schematically shown with arrows. Adapted from Ref. [30]. (A color version of this figure can be viewed online.)

are fibre spinning from CNTs in liquid solutions [21] and CNT fibre drawing directly from gaseous CNTs produced by floating catalysts [22]. Dry spinning is a third technique that consists in assembling fibres from vertically aligned CNTs without any additional handling steps in the process [23–25]. Basically, this corresponds to synthesizing CNTs with unique density and length. In the dry spinning process, Van der Waals interactions bind the CNTs together, allowing the array to be continuously drawn. The main advantage of this technique is the catalyst-free high alignment, and a smaller diameter distribution of the CNTs within the thread [23,26].

Various researchers have addressed the strength vs. toughness problem using CNT-based fibres. Dalton et al. produced composite fibres from polyvinyl alcohol (PVA) and about 60% by weight Single-Wall CNT (SWCNT), achieving a strength of 1.8 GPa and toughness of 570 J/g [27]. The fibres produced in Ref. [28], also based on PVA and SWCNT, reached an even higher value of 870 J/g, and the technique was also demonstrated for Multi-Wall CNTs (MWCNT), although with reduced strength and toughness values.

An approach to obtain artificial fibres that are simultaneously strong and tough is to try to replicate the mechanisms that are occurring at nano- micro- and macro-scale levels in natural

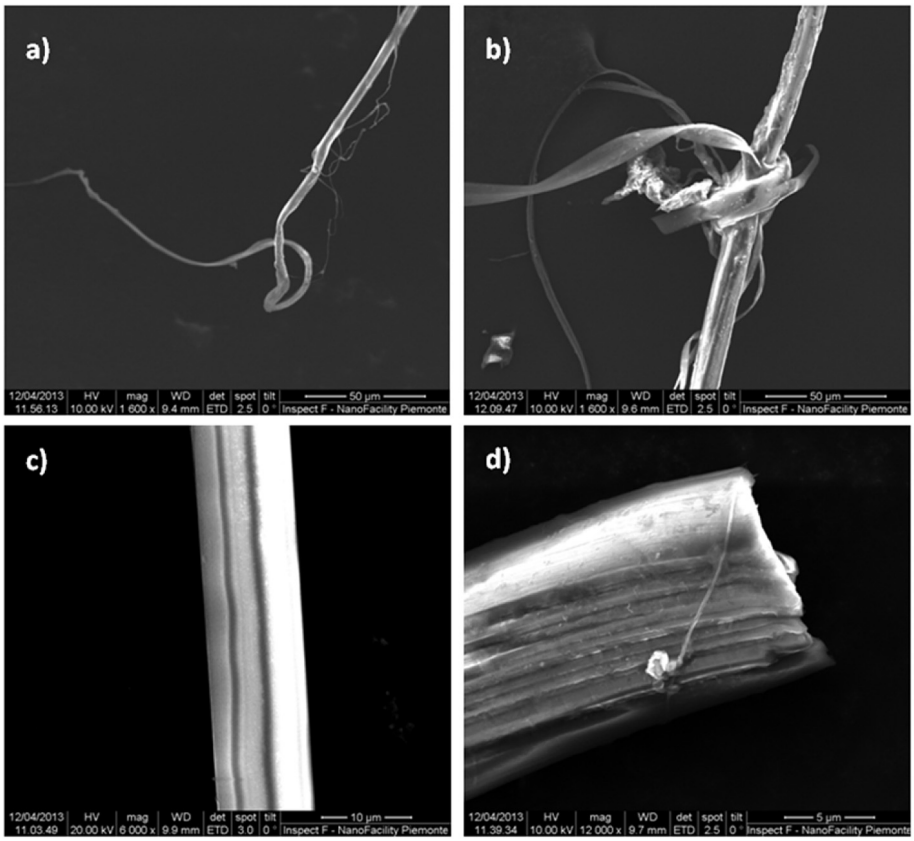

Fig. 2. SEM micrographs of some of the tested polymeric microfibres: a) fractured Kevlar® strand; b) knotted Kevlar® fibre undergoing degradation during slip; c) close-up of a Zylon® fibre; d) clean fracture on a Zylon® fibre.

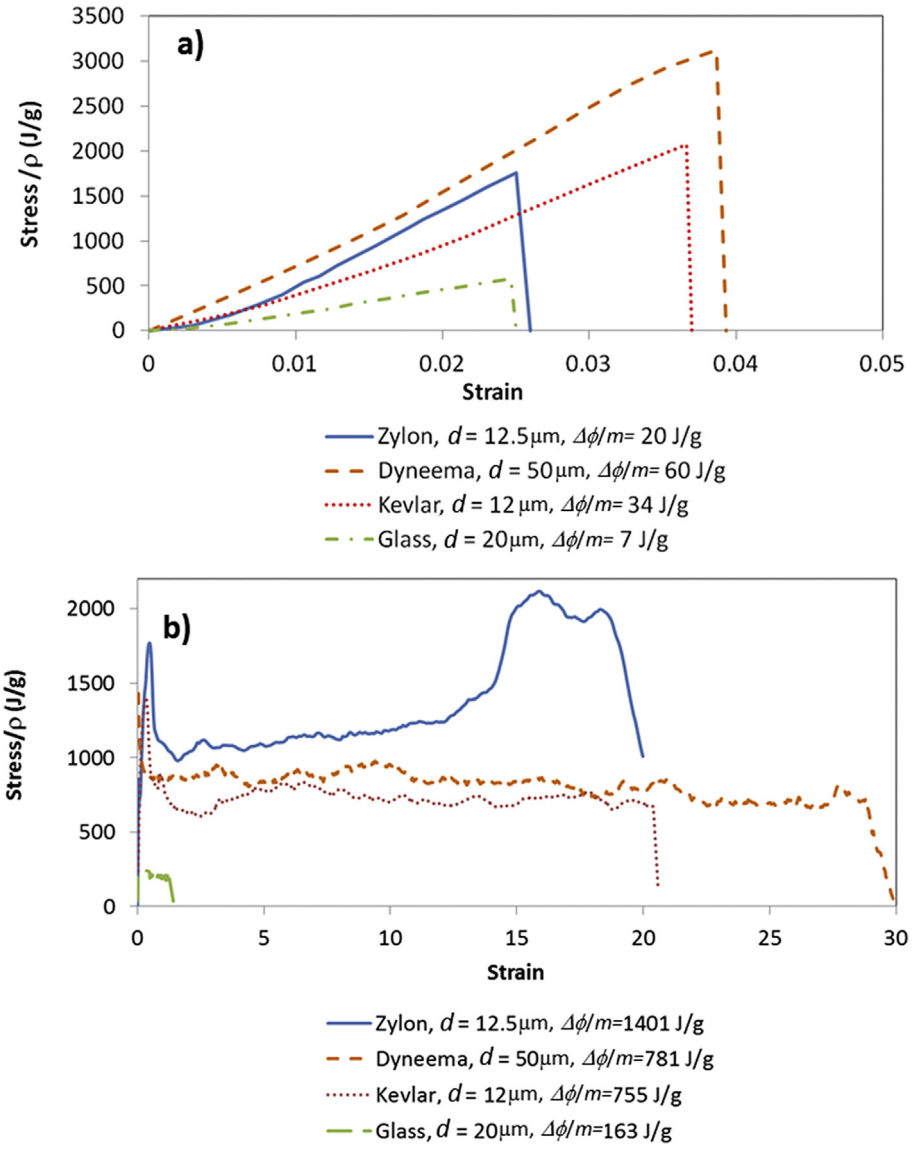

Fig. 3. Stress-strain curves for micro-tensile tests on Zylon®, Dyneema®, Kevlar® and Glass micro-fibres tested in a) unknotted and b) knotted configuration. The total dissipated energy per unit mass (toughness modulus) for each curve, as well as fibre diameter, is indicated in the legend. With the micro-fibre of Zylon® and the proposed strategy we well surpassed the previous toughness world record obtained at the macroscale, which was marginally above 1000 J/g [29]. (A color version of this figure can be viewed online.)

materials and structures such as spider silks and webs to enhance toughness, i.e. to introduce energy dissipation mechanisms without significantly reducing the overall fibre strength. This strategy has recently been proposed by Pugno [29], introducing the concept sliding elements such as of knots into fibres as frictional energy dissipators to mimic spider web junctions and obtaining toughness values above 1000 J/g. The concept was also applied to silk fibroin fibres in Ref. [30]. It can be shown that the resulting toughness of a knotted fibre, defined as the dissipated energy at break per unit mass $\Delta\phi/m$, can be expressed as.

$$\Delta\phi/m \approx k_1 k_2 k_3 \sigma_f \Big/ \rho \tag{1}$$

where ρ is the material mass density and k_1, k_2, k_3 are geometrical/mechanical parameters of the fibre/knot, all of which are comprised between 0 and 1: $k_1 = (l\text{-}l_0)/l$ is a knot parameter that relates the original fibre length l to its length l_0 after having introduced a knot; $k_2 = \sigma_k/\sigma_f$ is a parameter that quantifies fibre "fragilization", i.e. the strength reduction of the fibre from its original value σ_f to that after having introduced the knot σ_k; $k_3 = \sigma_p/\sigma_k$ is a parameter that measures the efficiency of the knot, as the ratio between the stress plateau σ_p in the stress-strain curve during sliding of the fibre in the knot, and the knotted fibre strength σ_k. From Eq. (1) we deduce that a fibre can ideally retain its "unknotted" strength, while acquiring an enhanced toughness of up to $\Delta\phi/m = \sigma_f/\rho$, where ρ is the fibre mass density, i.e. the toughness can be as large as the specific strength of the material. In Ref. [29], macroscopic synthetic polymer fibres were considered, finding consistent toughness improvements, surpassing for the first time 1000 J/g for an ultra-high-molecular-weight polyethylene (Dyneema®) fibre with multiple knots.

As is well known, a size reduction implies a variation in the critical defect distribution, and therefore a potential increase in fibre strength, albeit with an increased experimental difficulty in handling and testing the fibres. In this paper, we implement the concept of knots as dissipators in microfibres to reach unprecedented toughness enhancement values and prove the feasibility of the approach even at the micro-scale, considering both synthetic polymer microfibres (Section 2) and CNT fibres (Section 3).

2. Mechanical tests on synthetic polymeric micro-fibres

To begin, four different materials were chosen among the most commonly used high-performance micro-fibres: Glass, Kevlar®, Zylon® and Dyneema®. Carbon fibres were not considered due to their extreme fragility in bending, effectively making them impossible tie into knots. Single overhand knots were applied on the fibres so as to follow the criteria set out in Ref. [29], i.e. simultaneously maximizing k_1, k_2 and k_3 parameters. For example, varying degrees of tightening were applied to optimize the friction during sliding in the knot ($k_3 \rightarrow 1$), while avoiding excessive fibre degradation, i.e. without reducing the original strength ($k_2 \rightarrow 1$). A schematic of the knotting procedure is shown in Fig. 1.

The knots were applied to the chosen fibres, taking care not to damage them during handling. To perform the tensile tests in the desired loading range, an Agilent T150 Nanotensile testing system was used, which allows nN and nm sensitivity on loads and displacements, respectively. The samples, with a typical gauge length of 20 cm, were prepared in "C"-shaped paper frames and set-up in a clamped–clamped configuration in the sample holder. The paper frame was then cut and fibres loaded up to failure at a loading rate of 1 mm/min.

The micro-fibres were analysed before and after testing using a Scanning Electron Microscope (SEM) to exactly measure diameters, highlight surface features (which could be correlated to the friction behaviour) and observe fractured fibres after tensile tests to infer damage mechanisms. Some examples of the acquired images are shown in Fig. 2, also highlighting micro-fibre fragilization due to the damage during sliding in the knotted configuration. For example, in the case of Kevlar® fibres, degradation was observed during sliding before fracture (Fig. 2a and b), while little or no damage was observed in Zylon® fibres, with a clean fibre fracture away from the knot (Fig. 2d).

Typical results for mechanical tensile tests are shown in Fig. 3, for the (a) unknotted and (b) knotted configurations, respectively. Unknotted fibres showed an approximately linear stress-strain behaviour up to failure, which occurred between 2.5 and 4% strain. All specimens displayed a higher specific strength than the corresponding Dyneema® and Endumax® macro-fibres [29], i.e. between 2.5 and 3 GPa cm^3/g, except in the case of glass fibres (1.5 GPa cm^3/g). Knotted fibres, on the other hand, displayed an initial peak in the stress-strain curve, at the onset of fibre slipping in the knot, a subsequent plastic-like stress "plateau" where energy dissipation occurred due to sliding friction, and final failure at extremely high apparent strain values, i.e.: about 2000% in Zylon® and Kevlar® and up to 3000% for Dyneema®. Strain in this case is defined as $\varepsilon = x/l_0$, in relation to the knotted fibre length l_0, hence the term "apparent". In all of the tested fibre types, the energy dissipation plateau occurred for stress values close to the fibre strength (up to or above 50%), indicating a close-to optimized knot configuration. Correspondingly, an even greater increase in specific dissipated energy before fibre break was achieved with respect to the Endumax® tape in Ref. [29]: a 7000% improvement in the case of Zylon®, 1300% for Dyneema®, 2220% for Kevlar®, 2330% for Glass, respectively. In particular, a record value of 1401 J/g was obtained in the case of Zylon® micro-fibres, which is considerably higher than all the previous values reported in the published literature, confirming the efficiency of the idea proposed in [29].

3. Mechanical tests on CNT micro-fibres

3.1. Preparation of CNT fibres

CNT fibres were prepared using the dry-spinning method, as illustrated in Fig. 4, starting from the synthesis of spinnable vertically aligned CNTs. The multi-walled CNTs used for this work were

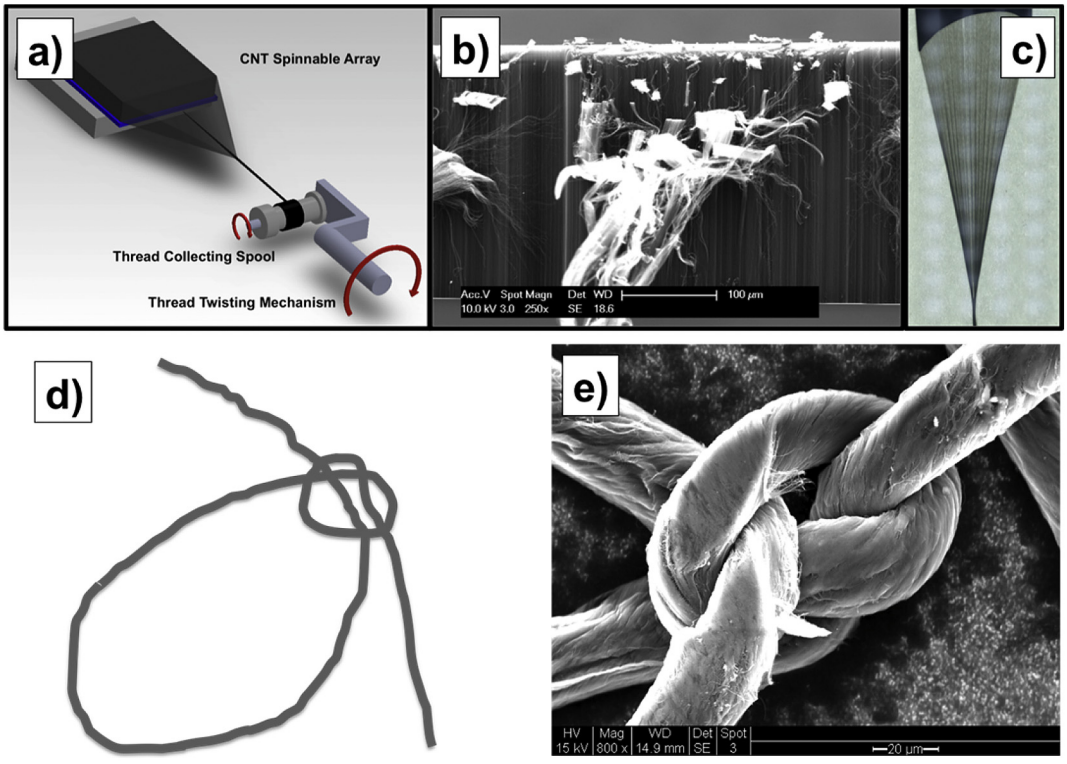

Fig. 4. (a) Scheme illustrating the CNT fibre spinning from drawable CNT arrays by combining translation and rotation of the fibre, and (b) SEM image of vertically aligned CNT array used for the CNT fibre spinning. (c) Optical image of the CNT fibre spinning from vertically aligned CNTs. (d) Scheme that illustrates a micro-slipknot. (e) SEM images of a typical micro-knot of CNT thread. (A color version of this figure can be viewed online.)

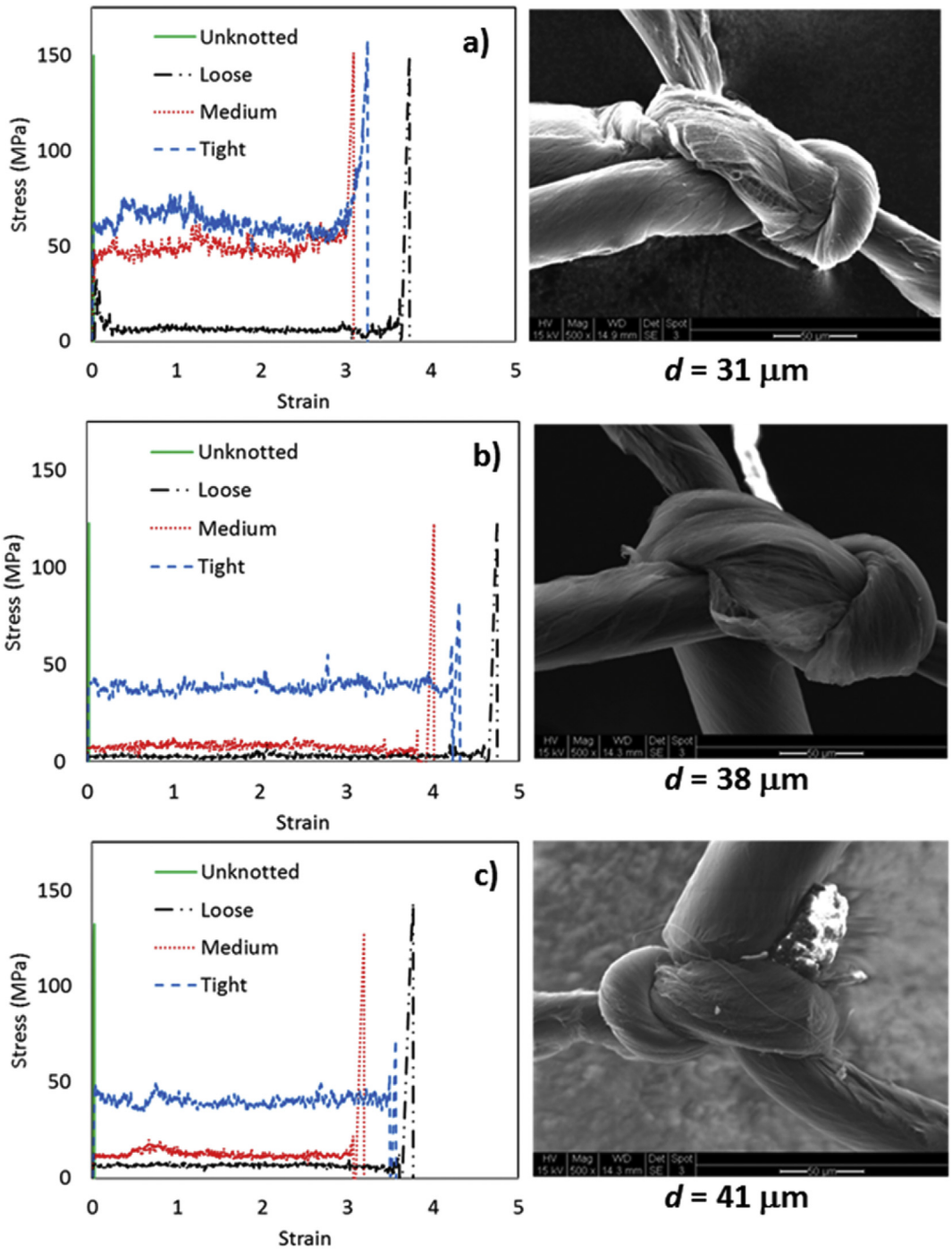

Fig. 5. Stress-strain curves up to failure for CNT threads with micro-slipknots on three different diameter CNT fibres and for different levels of tightening. Diameters are: a) $d = 31$ μm; b) $d = 38$ μm; c) $d = 41$ μm. (A color version of this figure can be viewed online.)

synthesized in accordance with previously reported procedures [31]. The as-synthesized CNT arrays were spun into yarns, also called fibres, by drawing a CNT bundle from the array. The spinnable CNT arrays were characterized by making a continuous bundle by grabbing with tweezers and pulling one side of the vertically aligned CNTs from the array. To ensure a constant pulling speed, the bundle was attached to a 8 mm bobbin which was fixed into the shaft of an electrical motor, whose rotation speed was controlled by the supplied electrical current. A twist was also applied to the drawn CNT web as illustrated in Fig. 4a. The typical length of the individual CNTs in the spinnable array is 450 μm, as shown in Fig. 4b. Fig. 4c shows an image of the array and the fibre at the twisting sites.

Fibre twist was applied to the drawn CNTs so as to form a uniform cylindrical shaped thread. The fibres were prepared with different twist angles, and with varying diameters for constant twist angles. Different twist angles were obtained by varying the draw and rotation speed while the array width was kept constant. The uniform width of the synthesized CNT arrays was ensured by the rectangular shape of the utilized Si wafer substrates. High twist

Table 1
Mechanical properties of the knotted and unknotted CNT fibres for different diameter values and levels of knot tightening, while keeping twist angles constant (columns 1–3, see Fig. 5), and for varying diameters and twist angles (columns 4–6, see Fig. 6).

	Thin Diameter	Medium Diameter	Thick Diameter	Low Twist Angle	Medium Twist Angle	High Twist Angle
Highest recorded Toughness for the knotted thread ($J.g^{-1}$)	93.3	89.2	102.6	53.4	103.8	96.8
Unknotted Thread Toughness ($J.g^{-1}$)	3.1	3.7	7.1	4.1	4.4	18.9
Strength to Density Ratio ($J.g^{-1}$)	298.2	348.6	474.5	529.3	405.8	340.0
Young's Modulus (GPa)	7.85	8.88	9.41	5.12	8.88	2.34
Diameter (μm)	31	38	41	41	31	30
Twist Angle (°)	24.5	24.5	24.5	18	24.5	46.5
Twist Rate (RPM)	913	913	913	760	913	1140
Draw Rate (RPM)	11	11	11	16	11	4
Array Width (mm)	10	16	18	10	10	10
Density ($g.cm^{-3}$)	0.53	0.35	0.30	0.28	0.30	0.49

angles were obtained by increasing the twist and decreasing the draw; conversely, low twist angles were obtained by decreasing the twist and increasing the draw. Variations in diameter were obtained by varying the width of the substrates and arrays of CNTs where the thread was drawn from (Fig. 4). The draw and twist rates were held constant resulting in similar twist angles in all threads with varying diameter. The diameter used in calculations was the average diameter over 20 measurements along the thread imaged with a Keyence digital microscope.

Since the CNTs were assembled without any foreign solvent interaction, the resulting thread was fairly porous with many internal voids, making it difficult to handle and detrimentally affecting the strength of the thread. To alleviate these problems, the thread was densified dipping into the organic solvent N-methyl-2-pyrrolidone (NMP) for 30 min. This caused air bubbles to rise to the surface. It is presumed that capillary forces of the solvent (NMP) draw the individual CNTs closer to each other and as a result the cross section of the CNT thread is reduced. The process resulted in the fibres having an approximate 30% diameter reduction with respect to the original, while densifications in acetone produced a 24% diameter reduction [32].

The afore-mentioned solvent densification typically improved the thread's overall tensile strength and made it easier to handle when adding knots with varying tightness. However, after solvent densification, the CNT thread still maintained radial compressibility, which was utilized in determining the tightness of the knot, by comparing the diameter of the thread before and after it was drawn through the micro slip-knot: tighter slip-knots produced smaller fibre diameters compared to loosely made slip-knots.

Experimental twist angles were determined by measuring the angles of the CNT alignment with a line traced parallel to the edges and located at between the edges. The traces for angle determination were performed on high-resolution SEM images and the angles were compared to the theoretical twist angle based on the equation $\varphi = \arctan(\pi \cdot d \cdot T \times 10^{-6})$, where φ is the surface twist angle, d (μm) is the diameter, and T (turns/m) is the twist.

3.2. Tensile tests

Overhand micro slip-knots (scheme shown in Fig. 4d) with one or two loops were then added to each of the threads, with each type of thread having a manually prepared loose, medium, or tight micro slip-knot. A SEM image is shown in Fig. 4e, where a single micro slip-knot is made by the thread starting at the top-right hand corner and ending at the bottom-left corner. A micro slip-knot with two loops was used when making tight slip-knots since a single loop slip-knot would loosen after it was tightened.

As previously, for tensile testing of CNT fibres, the ends of each fibre were glued onto a paper frame and experiments were conducted in an Instron tensile testing machine at a strain rate of 5 mm/min and using an active gauge length of 10 mm. All measurements were performed on threads from the same array

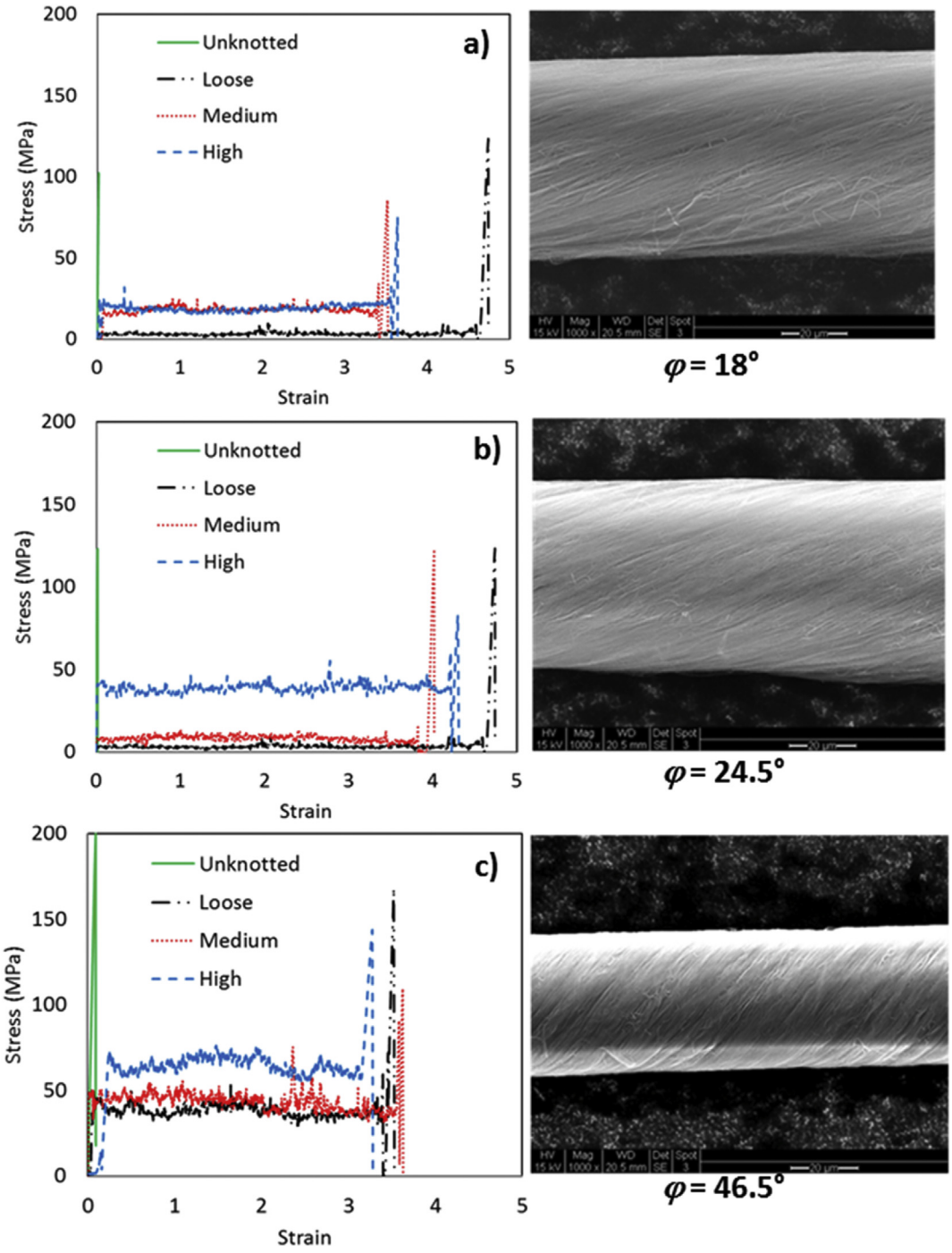

Fig. 6. Stress-strain curves up to failure for CNT threads with micro-slip knots using three different twist angles: a) $\varphi = 18°$; b) $\varphi = 24.5°$; c) $\varphi = 46.5°$. (A color version of this figure can be viewed online.)

and with the same CNT array width.

The tests were performed with the objective of achieving toughness improvements on CNT fibres as a function of various parameters. The tests were carried out for: (i) three different diameter values and similar superficial twist angles; (ii) three different twist angles and (iii) three different tightening levels on the micro slip-knots.

The measured stress-strain curves for specimens with fibre diameters varying between 31 μm and 41 μm are shown in Fig. 5a–c and the corresponding Young's modulus, specific strength and toughness are summarized in the first three columns of Table 1. Three different tightening levels were investigated, while the twist angle per unit length was kept constant at 24.5°. Other fibre spinning parameters such as twist rate, draw rate, array width are also included in the Table. As previously, the stress-strain curves for the knotted fibres displayed long plateau regions extending to high strain values (300%–400%) where energy dissipation takes place. As a consequence, in the presence of knots the toughness values increased by more than an order of magnitude, between 15 and 30 times the original values, reaching a highest value of 102.6 J/g. Note

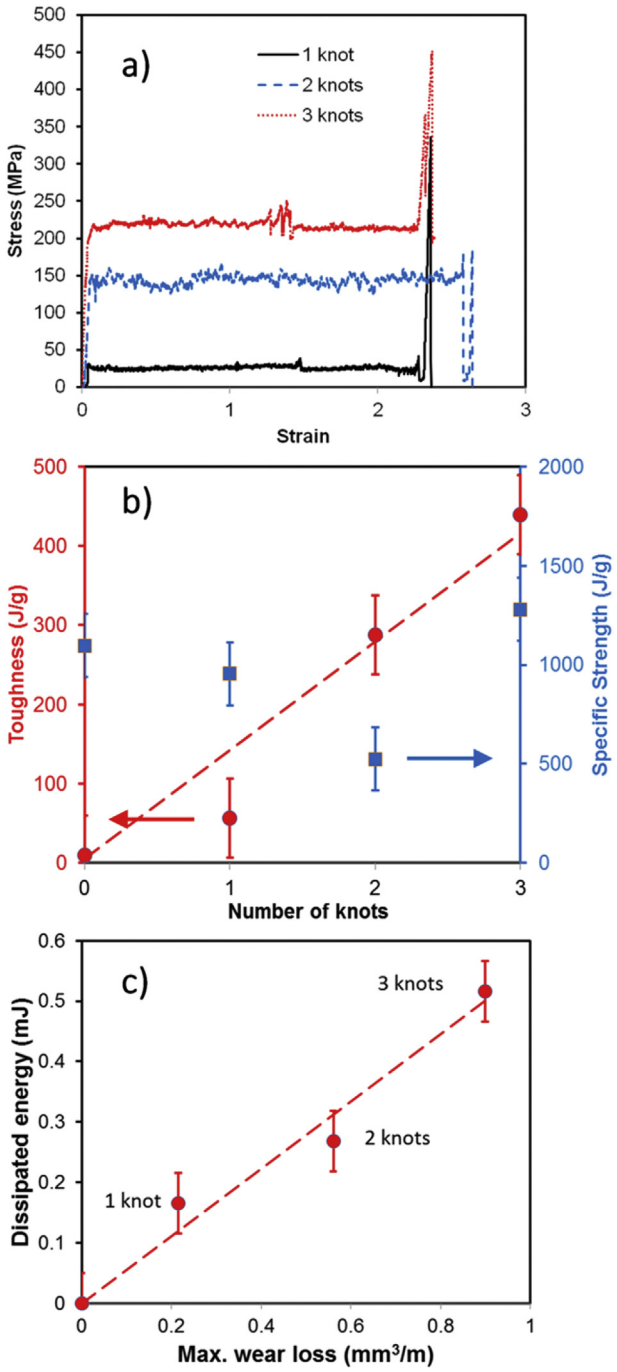

Fig. 7. a) Stress-strain curves up to failure for CNT threads with multiple micro-knots; b) Toughness and specific strength variation vs. number of micro-knots in the fibres; c) Dissipated energy in friction as a function of maximum wear loss for fibres with multiple micro-knots. (A color version of this figure can be viewed online.)

that toughness is no longer equal to the area under the stress-strain curve [29]. At the same time, fibre strength values remained virtually unchanged, with or without the knots, indicating that there was little fibre fragilization in the sliding phase (SEM images of the knots in the three fibres are also shown in Fig. 5). The influence of fibre diameter was relatively small, although results seemed to indicate that smaller diameters could provide better strength but smaller stiffness. On the other hand, there was a strong dependence on knot tightening, as can be seen in Fig. 5: a high energy-dissipation stress plateau (close to 50% the fibre strength) was achieved only in the tightest knot configurations.

The dependence on fibre twist was also investigated, and the corresponding stress-strain results are shown in Fig. 6a and b, while the resulting mechanical properties and drawing conditions are summarized in the last three columns of Table 1. Again, the addition of knots improved the fibre toughness by 5–24 times the original values, with a maximum of 103.8 J/g, while leaving the fibre strength virtually unchanged. The data seem to indicate that larger twist angles provide higher toughness. This could be possibly due to a higher internal friction of CNTs within the thread at higher twisting angles, which would increase specific strength and therefore toughness, due to internal friction. Another reason could be an increase in the friction of the fibre sliding in the knot for greater twist angles. Results in Fig. 6 again show that the tightening of the knot is crucial for obtaining high toughness. However, for high twist angles, knot tightening plays a reduced role, since friction efficiency is on average higher than for low twist angles.

To assess the influence of the type of knot more quantitatively, the friction of the micro slip-knot was increased progressively by increasing the number coils forming it [29]. Thus, significantly greater toughness values were achieved, with better control. Fig. 7a shows the toughness and specific strength values corresponding to CNT threads with single, double and triple micro slip-knots. The increase in toughness is initially approximately proportional to the number of coils, due to the larger friction forces that can be achieved on the fibre by increasing the knot pressure. A similar monotonic dependence cannot be reliably established for fibre strength, as can be seen in Fig. 7b, but results show that an increase in number of knots does not necessarily lead to fibre weakening. In the best case, a maximum toughness value of 439 J/g is achieved, with a corresponding specific strength of 1280 J/g. These values correspond to an approximate increase of 50 times in toughness with respect to the unknotted CNT fibre, with an unvaried strength (within experimental uncertainty).

The effect of multiple coils was also studied in separate experiments. Control of knot tightness was arduous, due to the small CNT fibre size, and therefore reduced visibility, difficult manipulation, and risk of fibre damage. However, indications regarding knot tightness could be obtained by monitoring the diameter reduction of the threads passing through the knot: average diameter reductions of 10%, 21% and 36% were obtained for 1, 2 and 3 coils, respectively. These values are partially indicative of higher pressure with an increasing number of coils, and possibly a higher contact area, leading to greater friction forces and an increase in overall toughness, but also of enhanced wear [33]. The latter hypothesis is supported by the observation in SEM images of CNTs accumulating on the knot surface. Assuming that the diameter reduction is due exclusively to wear, it is possible to deduce an upper bound of the wear loss WL per unit dissipated energy due to frictional sliding $\Delta\phi$, as shown in Fig. 7c. The dependence between WL and $\Delta\phi$ is approximately linear, so that the ratio between dissipated energy and wear loss $\Delta\phi/WL$ can be taken as the characteristic wear resistance WR of the system, finding $WR = (0.56 \pm 0.01)$ mJ m/mm^3. To our knowledge, this is the first experimental estimation of wear resistance for a CNT fibre.

4. Conclusions

To summarize the results discussed in this paper and compare them with previous results in the literature on macrofibres with outstanding mechanical properties, we have represented them in a toughness vs. strength plot in Fig. 8. Specific strength is considered, in order to compare materials with different densities. The plot highlights the huge increase in toughness, (roughly two orders of magnitude) that can be achieved through the use of slip-knots as

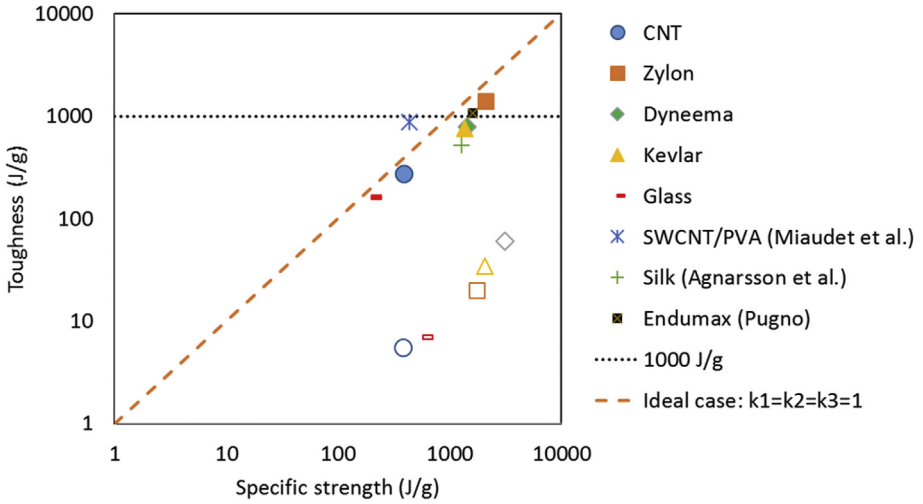

Fig. 8. Summary of toughness vs. specific strength values obtained in this paper, compared to previous outstanding results in the literature: silk [7], SWCNT/PVA [17], or Endumax [29]. The 1000 J/g toughness level (dotted line) and the toughness limit using a knot (dashed line) are provided as a reference. The plot demonstrates how using knots as energy dissipators [29] allows an increase of 2 orders of magnitude in toughness, regardless of the material. Zylon® microfibres achieve the highest values to date, but CNT fibres, as considered in this work, could ideally surpass this, if sufficiently high strength values are achieved and knot dissipation optimized. (A color version of this figure can be viewed online.)

energy dissipators. This strategy has allowed us to obtain in Zylon® microfibres the highest toughness value to date for any given fibre.

The figure also shows that high-strength values are a prerequisite for high toughness values when using knotted fibres, in accordance with Eq. (1). This is in contrast with the usual behaviour of artificial materials, where strength and toughness are competing properties. This consideration immediately leads us to consider CNTs as ideal candidates for the realization of fibres with maximal strength and toughness. With this in mind, we have successfully demonstrated the experimental feasibility of using slipknots in CNT fibres, proving that fibre degradation is minimal and that the knots can be introduced in a controlled and repeatable fashion, which also allows parameter optimization, such as fibre twist or diameter, to maximize the desired properties. Experiments also allow the estimation for the first time of the wear resistance of CNT fibres.

The next step will be to adopt the same strategy with higher strength CNT, Graphene or other 2D material fibres, or in composite synthetic polymer fibres reinforced with the previously mentioned materials. Improved knot topology or more complicated sliders could also be considered to optimize toughness enhancement. This should allow us to further optimize mechanical properties and fully exploit the potential of the proposed idea [29], thus opening the way to its full application in fibre-related technologies in various industrial sectors (e.g., sporting goods, automotive, aerospace, protective devices).

Acknowledgements

N.M.P. was supported by the ERC (StG Ideas 2011 No. 279985 BIHSNAM, PoC 2013-2 No. 632277 KNOTOUGH, ERC PoC 2015 SILKENE no. 693670), by the EC Graphene Flagship (WP10, No. 604391), and by the Provincia Autonoma di Trento ("Graphene nanocomposites," No. S116/2012–242637 and reg. delib. No. 2266). E.L. and F.B. were supported by BIHSNAM. N.T.E., P.M. and V.S. are grateful to Nicholas Kienzle, Rachit Malik and Mark Hasse for their suggestions and comments related to this project, and acknowledge the funding agencies: NSF through GOALI grant 1120382 and NSF grant CMMI-07272500 from NCA&T, a DURIP-ONR grant, and ERC supplemental STTR funded by NSF (2010–2012).

Appendix A. Supplementary data

Supplementary data related to this article can be found at http://dx.doi.org/10.1016/j.carbon.2016.02.025.

References

[1] E.R. Dumont, Bone density and the lightweight skeletons of birds, P Roy. Soc. B-Biol. Sci. 277 (1691) (2010) 2193–2198.
[2] U.G.K. Wegst, H. Bai, E. Saiz, A.P. Tomsia, R.O. Ritchie, Bioinspired structural materials, Nat. Mater. 14 (1) (2015) 23–36.
[3] R.O. Ritchie, The conflicts between strength and toughness, Nat. Mater. 10 (11) (2011) 817–822.
[4] M. Yahyazadehfar, D. Bajaj, D.D. Arola, Hidden contributions of the enamel rods on the fracture resistance of human teeth, Acta Biomater. 9 (1) (2013) 4806–4814.
[5] F. Barthelat, Nacre from mollusk shells: a model for high-performance structural materials, Bioinspir. Biomim. 5 (3) (2010).
[6] J.C. Weaver, G.W. Milliron, A. Miserez, K. Evans-Lutterodt, S. Herrera, I. Gallana, et al., The stomatopod dactyl club: a formidable damage-tolerant biological hammer, Science 336 (6086) (2012) 1275–1280.
[7] Z.Z. Shao, F. Vollrath, Materials: surprising strength of silkworm silk, Nature 418 (6899) (2002), 741-.
[8] I. Agnarsson, M. Kuntner, T.A. Blackledge, Bioprospecting finds the toughest biological material: extraordinary silk from a giant riverine orb spider, Plos One 5 (9) (2010).
[9] N.M. Pugno, The design of self-collapsed super-strong nanotube bundles, J. Mech. Phys. Solids 58 (9) (2010) 1397–1410.
[10] N.M. Pugno, The role of defects in the design of space elevator cable: From nanotube to megatube, Acta Mater. 55 (15) (2007) 5269–5279.
[11] M.F. Yu, B.S. Files, S. Arepalli, R.S. Ruoff, Tensile loading of ropes of single wall carbon nanotubes and their mechanical properties, Phys. Rev. Lett. 84 (24) (2000) 5552–5555.
[12] M.F. Yu, O. Lourie, M.J. Dyer, K. Moloni, T.F. Kelly, R.S. Ruoff, Strength and breaking mechanism of multiwalled carbon nanotubes under tensile load, Science 287 (5453) (2000) 637–640.
[13] C. Lee, X.D. Wei, J.W. Kysar, J. Hone, Measurement of the elastic properties and intrinsic strength of monolayer graphene, Science 321 (5887) (2008) 385–388.
[14] H.I. Rasool, C. Ophus, W.S. Klug, A. Zettl, J.K. Gimzewski, Measurement of the intrinsic strength of crystalline and polycrystalline graphene, Nat. Commun. 4 (2013).
[15] Z. Xu, H.Y. Sun, X.L. Zhao, C. Gao, Ultrastrong fibers assembled from giant graphene oxide sheets, Adv. Mater. 25 (2) (2013) 188–193.
[16] N.M. Pugno, On the strength of the carbon nanotube-based space elevator cable: from nanomechanics to megamechanics, J. Physics-Condensed Matter 18 (33) (2006) S1971–S1990.
[17] N.M. Pugno, F. Bosia, A. Carpinteri, Multiscale stochastic simulations for tensile testing of nanotube-based macroscopic cables, Small 4 (8) (2008) 1044–1052.

[18] L.Q. Liu, W.J. Ma, Z. Zhang, Macroscopic carbon nanotube assemblies: preparation, properties, and potential applications, Small 7 (11) (2011) 1504–1520.
[19] W.B. Lu, M. Zu, J.H. Byun, B.S. Kim, T.W. Chou, State of the art of carbon nanotube fibers: opportunities and challenges, Adv. Mater. 24 (14) (2012) 1805–1833.
[20] N. Behabtu, M.J. Green, M. Pasquali, Carbon nanotube-based neat fibers, Nano Today 3 (5–6) (2008) 24–34.
[21] N. Behabtu, C.C. Young, D.E. Tsentalovich, O. Kleinerman, X. Wang, A.W.K. Ma, et al., Strong, light, multifunctional fibers of carbon nanotubes with ultrahigh conductivity, Science 339 (6116) (2013) 182–186.
[22] K. Koziol, J. Vilatela, A. Moisala, M. Motta, P. Cunniff, M. Sennett, et al., High-performance carbon nanotube fiber, Science 318 (5858) (2007) 1892–1895.
[23] K.L. Jiang, J.P. Wang, Q.Q. Li, L.A. Liu, C.H. Liu, S.S. Fan, Superaligned carbon nanotube arrays, films, and yarns: a road to applications, Adv. Mater. 23 (9) (2011) 1154–1161.
[24] M. Zhang, K.R. Atkinson, R.H. Baughman, Multifunctional carbon nanotube yarns by downsizing an ancient technology, Science 306 (5700) (2004) 1358–1361.
[25] K.L. Jiang, Q.Q. Li, S.S. Fan, Nanotechnology: spinning continuous carbon nanotube yarns – carbon nanotubes weave their way into a range of imaginative macroscopic applications, Nature 419 (6909) (2002) 801.
[26] K.R. Atkinson, S.C. Hawkins, C. Huynh, C. Skourtis, J. Dai, M. Zhang, et al., Multifunctional carbon nanotube yarns and transparent sheets: fabrication, properties, and applications, Phys. B 394 (2) (2007) 339–343.
[27] A.B. Dalton, S. Collins, E. Munoz, J.M. Razal, V.H. Ebron, J.P. Ferraris, et al., Super-tough carbon-nanotube fibres–these extraordinary composite fibres can be woven into electronic textiles, Nature 423 (6941) (2003) 703.
[28] P. Miaudet, S. Badaire, M. Maugey, A. Derre, V. Pichot, P. Launois, et al., Hot-drawing of single and multiwall carbon nanotube fibers for high toughness and alignment, Nano Lett. 5 (11) (2005) 2212–2215.
[29] N.M. Pugno, The “egg of columbus” for making the world's toughest fibres, Plos One 9 (4) (2014).
[30] A. Berardo, M.F. Pantano, N.M. Pugno, Slip knots and unfastening topologies enhance toughness without reducing strength of silk fibroin fibres, Interface Focus 6 (2016) 20150060.
[31] C. Jayasinghe, S. Chakrabarti, M.J. Schulz, V. Shanov, Spinning yarn from long carbon nanotube arrays, J. Mater. Res. 26 (05) (2011) 645–651.
[32] L. Kai, S. Yinghui, Z. Ruifeng, Z. Hanyu, W. Jiaping, L. Liang, et al., Carbon nanotube yarns with high tensile strength made by a twisting and shrinking method, Nanotechnology 21 (4) (2010) 045708.
[33] K. Friedrich, A.K. Schlarb, Tribology of Polymeric Nanocomposites : Friction and Wear of Bulk Materials and Coatings, first ed., Elsevier, Oxford; New York, 2008.

Supplementary Material

Knotted Synthetic Polymer or Carbon Nanotube Micro -Fibres with Enhanced Toughness

Federico Bosia, Emiliano Lepore, Noe T. Alvarez, Peter Miller, Vesselin Shanov, and Nicola M. Pugno[*]

CNT fibre densification

As discussed in the main text, CNT fibres were densified by dipping into the organic solvent N-methyl-2-pyrrolidone (NMP) for 30 minutes. The effect was to reduce the cross section of the CNT thread is reduced. The diameter reduction in NMP is shown in Figure S1 for ten samples measured with a digital microscope, providing an average diameter of 50.62 μm for pristine, and 35,53 μm for NMP densified CNT fibers, resulting in about 30% diameter reduction. Standard deviations of diameter variation 1.90 (pristine) and 2.29 (NMP-densified) are observed. NMP is known to be a better solvent than Acetone for CNTs, therefore higher densification results are expected, although in our case the difference among the two solvents are minimal.

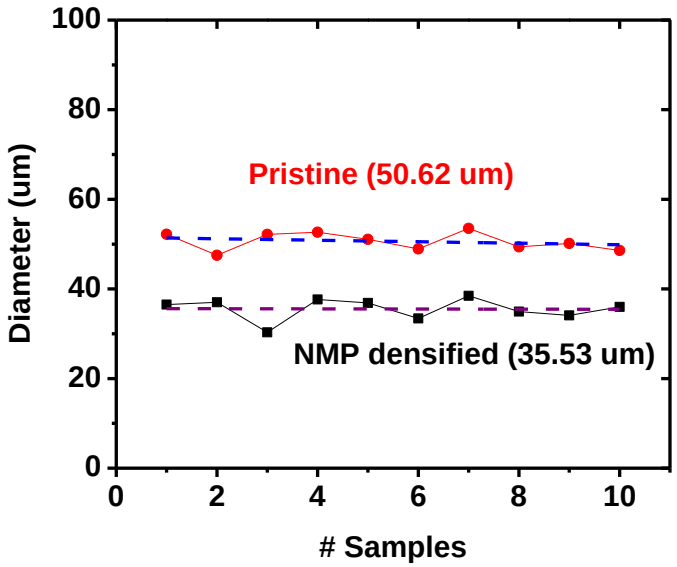

Figure S1: Measured diameters for pristine and NMP densified CNT fibers. An approximate 29.8% diameter reduction is observed.

Additional SEM images of CNT fibres

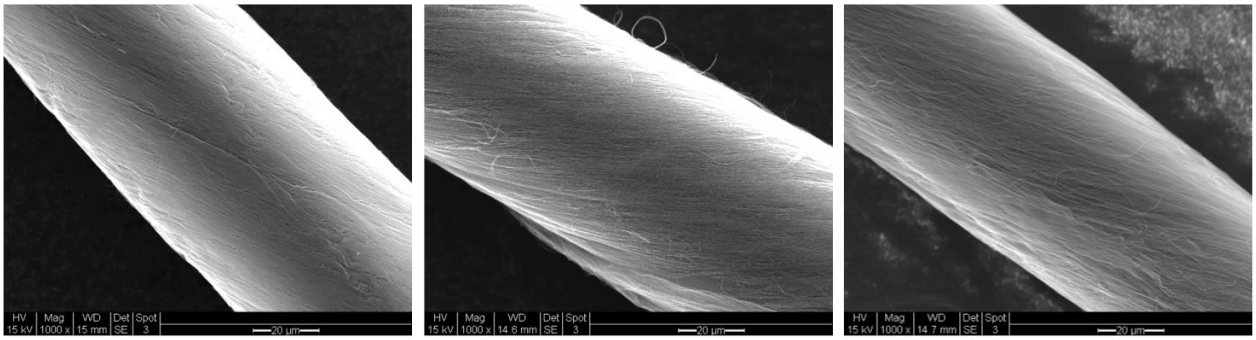

Figure S2: SEM images of three different diameter CNT fibres.

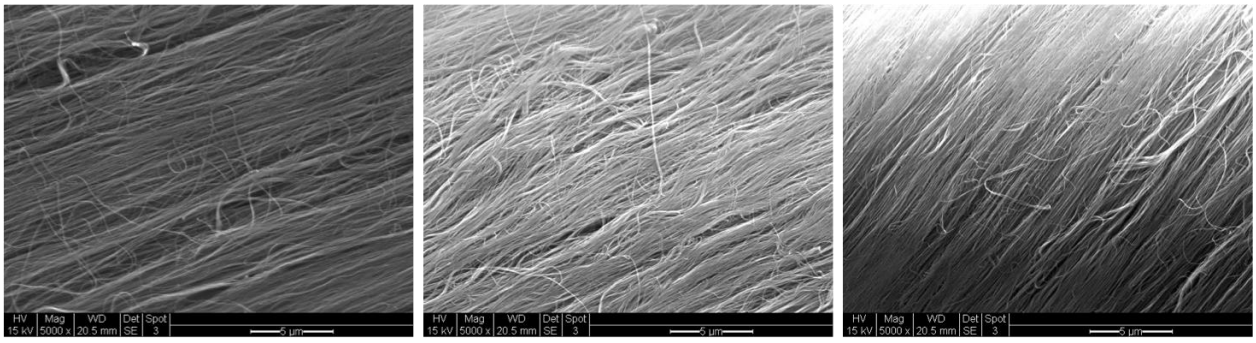

Figure S3: Enlarged SEM images of CNT fibres with nanotubes aligned in different twist angles with respect to an axial line along the fibre.

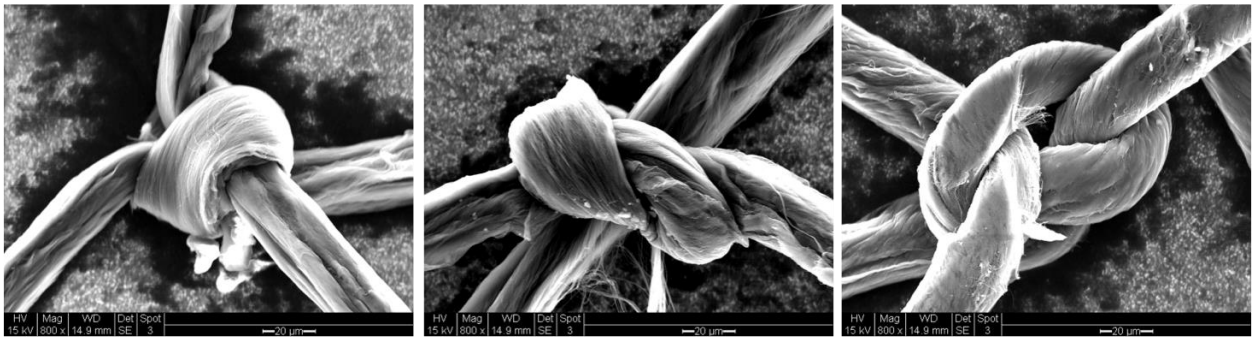

Figure S4: SEM images of the slipknots made of the three different twist angle CNT fibres

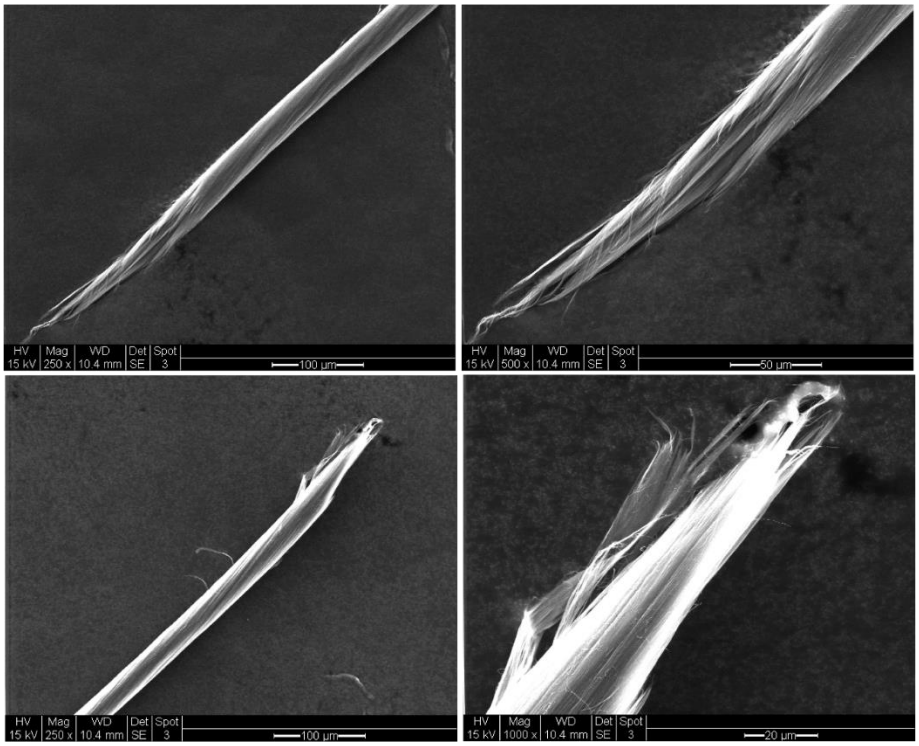

Figure S5: SEM images of NMP-densified CNT fiber fracture surfaces. Top and bottom images correspond to both ends of fractured CNT fiber.

Additional Video showing tensile testing of knotted Zylon fibre in a nanotensile tesing system, together with the corresponding stress-strain curve. Pulling speed is 0.5%/s.